JACS
JOURNAL OF THE AMERICAN CHEMICAL SOCIETY

pubs.acs.org/JACS

Article

Social Self-Sorting Synthesis of Molecular Knots

Zoe Ashbridge, Olivia M. Knapp, Elisabeth Kreidt, David A. Leigh,* Lucian Pirvu, and Fredrik Schaufelberger

Cite This: *J. Am. Chem. Soc.* 2022, 144, 17232−17240

Read Online

ACCESS | Metrics & More | Article Recommendations | Supporting Information

ABSTRACT: We report the synthesis of molecular prime and composite knots by social self-sorting of 2,6-pyridinedicarboxamide (pdc) ligands of differing topicity and stereochemistry. Upon mixing achiral monotopic and ditopic pdc-ligand strands in a 1:1:1 ratio with Lu(III), a well-defined heteromeric complex featuring one of each ligand strand and the metal ion is selectively formed. Introducing point-chiral centers into the ligands leads to single-sense helical stereochemistry of the resulting coordination complex. Covalent capture of the entangled structure by ring-closing olefin metathesis then gives a socially self-sorted trefoil knot of single topological handedness. In a related manner, a heteromeric molecular granny knot (a six-crossing composite knot featuring two trefoil tangles of the same handedness) was assembled from social self-sorting of ditopic and tetratopic multi-pdc strands. A molecular square knot (a six-crossing composite knot of two trefoil tangles of opposite handedness) was assembled by social self-sorting of a ditopic pdc strand with four (*S*)-centers and a tetratopic strand with two (*S*)- and six (*R*)-centers. Each of the entangled structures was characterized by ^{1}H and ^{13}C NMR spectroscopy, mass spectrometry, and circular dichroism spectroscopy. The precise control of composition and topological chirality through social self-sorting enables the rapid assembly of well-defined sequences of entanglements for molecular knots.

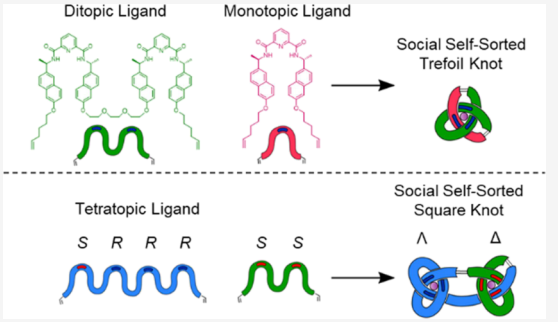

INTRODUCTION

Knots and entanglements are found at all length scales, from spontaneous random tangling of polymer chains to well-defined specialized climbing and sailing knots.[1] Self-entanglement of a molecular strand can cause changes in properties such as molecular volume and shape,[2] strain,[3] chiral expression,[4] and photophysical characteristics.[5] Relatively simple synthetic molecular knot topologies have proven efficacious in areas as diverse as catalysis,[6] mechanical barrier formation,[7] dopants for chiral materials,[8] and nanotherapeutics.[9]

However, accessing different molecular knot scaffolds remains challenging.[10−14] Single enantiomer[15] trefoil knots have been synthesized by coordination of three 2,6-pyridinedicarboxamide (pdc) ligands[14] containing asymmetrically substituted benzyl groups around a lanthanide(III) ion; the point chirality leads to stereoselective assembly of the ligands around the metal center.[14a,15] This, in turn, directs the topological chirality of the closed-loop knot that results from covalent capture of the complex by ring-closing olefin metathesis[16] (RCM).

Molecular trefoil knots have been synthesized by the folding and threading of a single tritopic ligand strand[17,18] (including those containing three pdc units[18]) around a metal ion template, reminiscent of the familiar way that knots are tied in our everyday world. This generates robust trefoil knot precursors ("tangles"[1a,c]) with unjoined strand ends, so-called overhand knots.[17−20] Enantiopure overhand knots[18] can be used for the synthesis[20] of composite[19−21] knots, joining together two tangles of either the same (3_1#3_1 granny knots) or opposing (3_1#*3_1 square knots) handedness.[20] However, such syntheses require linear synthetic schemes that may be lengthy and result in low overall yields.[19,20]

A useful synthetic strategy for rapidly assembling complexity from simple building blocks is self-sorting.[22] Self-sorting systems can either be narcissistic[23]—each component preferring to interact with others like themselves—or social,[24] whereby a compound has greater affinity for components within a system that are different from itself. Narcissistic self-sorting is more common in artificial supramolecular systems, where it tends to yield simpler, high symmetry, homomeric assemblies.[25]

The synthesis of two 12-crossing composite triskelion knots via a Vernier template approach was recently reported.[18b] By using a coordinative mismatch of lanthanide(III) ions and pdc ligands of varying topicity, entangled assemblies containing the lowest common multiple total binding sites were formed. This

Received: July 20, 2022
Published: September 6, 2022

allowed for the synthesis of large composite knots from comparatively simple ligand precursors in relatively few synthetic steps.[18b] However, it also suggests a more general strategy for rapidly accessing complex higher-order entanglements. Here, we report the social self-sorting synthesis of prime and composite molecular knots, exemplified by the entropically driven synthesis of heteromeric trefoil, granny, and square knots.[26]

RESULTS AND DISCUSSION

Social Self-Sorting Synthesis of a Trefoil Knot Precursor Using Achiral Monotopic and Ditopic Building Blocks. A 1:1:1 mixture of monotopic ligand **L1**, ditopic ligand **L2**, and lutetium(III) ions could potentially form any of three distinct complexes: two narcissistically self-sorted homomeric helicates comprising three identical ligands, or a socially self-sorted heteromeric helicate featuring one of each ligand (Figure 1). In contrast to homomeric complexes

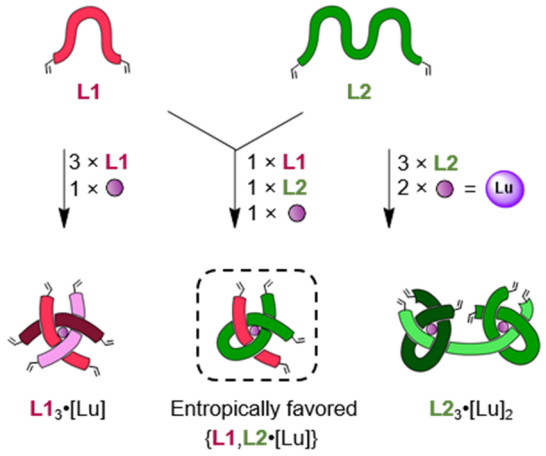

Figure 1. Social self-sorting of ligand strands of different topicity leads to favored heteromeric open knot complexes. Achiral monotopic ligand **L1** and achiral ditopic ligand **L2** form racemic heteromeric trefoil knot precursor {**L1**,**L2**·[Lu]} upon coordination to Lu(III), as this complex requires only two ligand strands to satisfy the lanthanide coordination sphere.

L1$_3$·[Lu] and **L2**$_3$·[Lu]$_2$, heteromeric complex {**L1**,**L2**·[Lu]} requires only two ligands per metal ion to satisfy the Lu(III) coordination requirements and should therefore be favored.

To assess this concept, first of all, homomeric complexes of each type of ligand coordinated to lutetium(III) were prepared (Scheme 1). Achiral monotopic ligand **L1** and ditopic ligand **L2** were synthesized as described in the Supporting Information (Scheme S2). Complexation of three equivalents of **L1** with one equivalent of lutetium(III) trifluoromethanesulfonate in acetonitrile afforded helicate **L1**$_3$·[Lu] upon heating to 80 °C for 2 h (Schemes 1i and S4).[14] The progress of the coordination process was monitored by electrospray ionization (ESI) mass spectrometry (Figure S77) and ^{1}H nuclear magnetic resonance (NMR) spectroscopy (Figure S48). Under similar reaction conditions, ditopic ligand **L2** was complexed to Lu(III) in a 3:2 ratio, generating complex **L2**$_3$·[Lu]$_2$ over 48 h (Schemes 1iii and S5). The ^{1}H NMR spectrum (Figure S2) and ESI mass spectrum (Figure S79) confirmed that an entangled species with 3:2 ligand:metal ratio had been formed.[18b]

We then investigated the propensity of **L1** and **L2** to self-sort into heteromeric coordination complexes. An acetonitrile solution containing a 1:1:1 mixture of **L1**, **L2** and lutetium(III) trifluoromethanesulfonate was heated at 80 °C (Scheme 1ii). After 20 h, the major ions in the ESI mass spectrum corresponded to the heteromeric complex {**L1**,**L2**·[Lu]}, with no evidence of homomeric complexes **L1**$_3$·[Lu] or **L2**$_3$·[Lu]$_2$ (Figure S81), indicating that the mixture does, indeed, socially self-sort to form the favored complex. Given the similarity in coordination chemistry of different lanthanides, it appears likely that the high selectivity observed originates mainly from entropic effects and, in particular, the number of species in each complex. Next, in order to use social self-sorting to control the crossing sequences more generally using this strategy, directors for entanglement stereochemistry were also introduced (Figure 2).[14,18]

Social Self-Sorting Synthesis of Trefoil Knots with Chiral Monotopic and Ditopic Building Blocks. To use point chirality to direct tangle stereochemistry within the self-sorted complexes, ditopic ligand (*R*)$_4$-**L4** and monotopic ligand (*R*)$_2$-**L3** were synthesized as described in the Supporting Information (Scheme S3). Homomeric complexes Λ-((*R*)$_2$-**L3**)$_3$·[Lu] and (Λ,Λ)-((*R*)$_4$-**L4**)$_3$·[Lu]$_2$ were prepared in an analogous manner to the reactions featuring the achiral building blocks (Scheme S7).[15] Addition of lutetium(III) trifluoromethanesulfonate (1 equiv) to a 1:1 mixture of (*R*)$_2$-**L3** and (*R*)$_4$-**L4** in acetonitrile resulted in the formation of heteromeric complex Λ-{(*R*)$_2$-**L3**,(*R*)$_4$-**L4**·[Lu]} after 24 h at 80 °C (Figure 2a).

The progress of the assembly process was monitored by ^{1}H NMR spectroscopy (Figure 2(bi–iii)) and ESI-MS (Figure 2c). The most abundant ions in the ESI mass spectrum (*m*/*z* Λ-{(*R*)$_2$-**L3**,(*R*)$_4$-**L4**·[Lu]}$^{3+}$ 711.3, Λ-{(*R*)$_2$-**L3**,(*R*)$_4$-**L4**·[Lu]}-H^{2+} 1066.4, Λ-{(*R*)$_2$-**L3**,(*R*)$_4$-**L4**·[Lu]}[CF$_3$SO$_3$]$^{2+}$ 1141.3) correspond to the heteromeric complex, while smaller signals arise from the homomeric circular helicate (*m*/*z* Λ-((*R*)$_2$-**L3**)$_3$·[Lu]$^{3+}$ 728.0, Λ-((*R*)$_2$-**L3**)$_3$·[Lu][CF$_3$SO$_3$]$^{2+}$ 1166.3) and open granny knot complex (*m*/*z* (Λ,Λ)-((*R*)$_4$-**L4**)$_3$·[Lu]$_2$[CF$_3$SO$_3$]$^{5+}$ 873.4) (Figure 2c). High-resolution mass spectrometry displays isotopic distributions for each complex consistent with the calculated values (Figure S84).

Diffusion-ordered NMR spectroscopy (DOSY) indicates a single species is present in solution (Figure 2d). The CD spectrum showed exciton couplings and signal intensities consistent with previously reported tangled pdc complexes (Figure S121).[14,15,18] Substantial upfield shifts of protons H$_A$ and H$_D$ in Λ-{(*R*)$_2$-**L3**,(*R*)$_4$-**L4**·[Lu]} (Figure 2b(iii)) result from shielding by the naphthalene rings and are consistent with an entangled conformation.[14] The splitting of the H$_A$ signals into different regions (~7.0 and 6.0 ppm) reflects the difference in the environments of their positions in the coordination complex. The pyridine protons at the open side of the complex (green pyridine sites) are less shielded than the more tightly bound (pink) sites internal to the structure.[4b] Additional splitting of each set of protons for H$_B$, H$_C$, and H$_D$ into chemically distinct environments also reflects the formation of the low-symmetry coordination complex, Λ-{(*R*)$_2$-**L3**,(*R*)$_4$-**L4**·[Lu]}.

The entangled complex Λ-{(*R*)$_2$-**L3**,(*R*)$_4$-**L4**·[Lu]} was covalently captured by RCM using a Hoveyda–Grubbs second generation catalyst to give the closed-loop trefoil knot Λ-**1**·[Lu] (Figure 2a). The ESI mass spectrum of the crude reaction mixture after RCM showed only ions corresponding to the

https://doi.org/10.1021/jacs.2c07682
J. Am. Chem. Soc. 2022, 144, 17232–17240

Scheme 1. Assembly of Achiral Complexes $L1_3$·[Lu], $L2_3$·$[Lu]_2$, and Socially Self-Sorted Complex {L1,L2·[Lu]}[a]

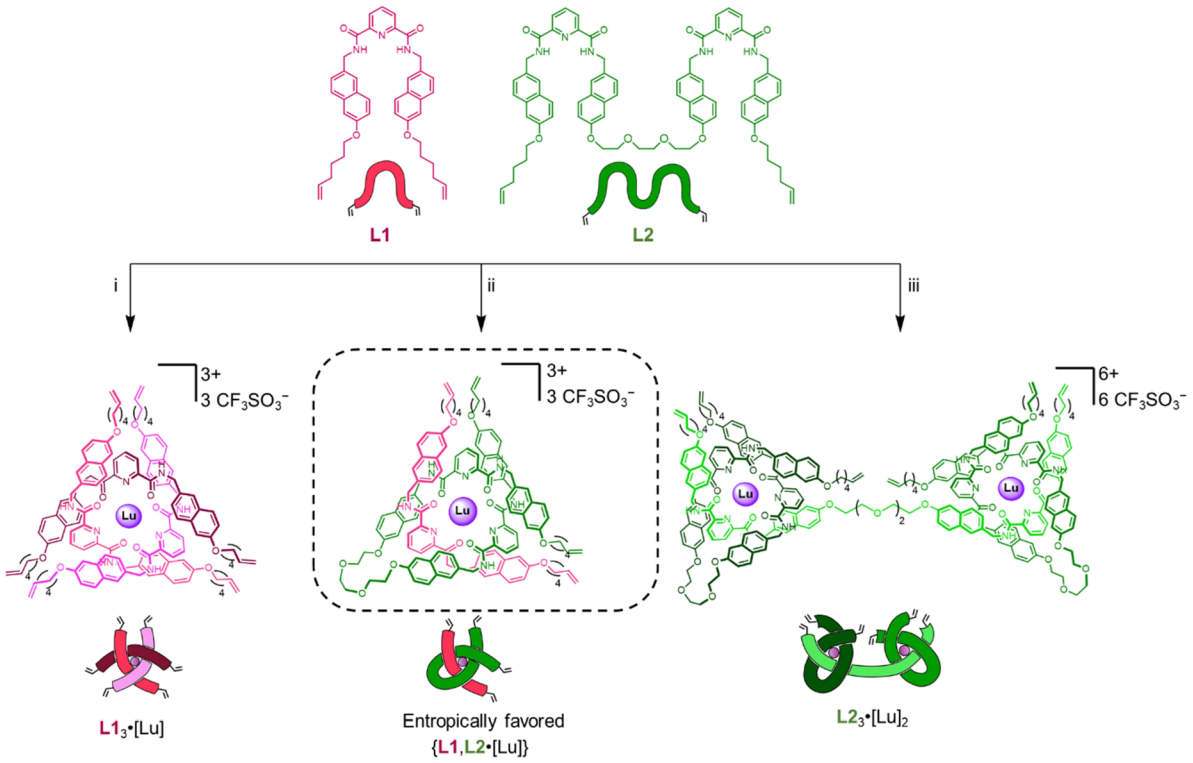

[a]Reagents and conditions: (i) 3× **L1**, $Lu(CF_3SO_3)_3$, MeCN, 80 °C, 2 h, 85%. (ii) **L1**, **L2**, $Lu(CF_3SO_3)_3$, MeCN, 80 °C, 20 h, 92%. (iii) 3× **L2**, 2× $Lu(CF_3SO_3)_3$, MeCN, 80 °C, 48 h, 82%.

desired knot, Λ-**1**·[Lu] (*m*/*z* Λ-**1**·$[Lu]^{3+}$ 692.7, Λ-**1**·[Lu]-H^{2+} 1038.4, Λ-**1**·[Lu]$[CF_3SO_3]^{2+}$ 1113.4), with no trace of assemblies derived from narcissistic self-sorting (Figure S3). The DOSY spectrum indicated a single species (Figure S72), and the CD spectrum confirmed that the entanglement stereochemistry is conserved in the closed-loop knot (Figure S109). Purification by size exclusion chromatography removed small amounts of unreacted starting material and larger molecular weight species to give trefoil knot Λ-**1**·[Lu] in 53% yield over two steps (Scheme S8). The modest isolated yield results from the oligomeric and polymeric side products from alkene metathesis and the loss of some of the poorly soluble knot during chromatography.

The ^{1}H NMR spectrum of Λ-**1**·[Lu] shows the absence of terminal alkenes (Figure 2b(iv)). The narrower range of chemical shifts of H_A with respect to the open complex (Λ-{$(R)_2$-**L3**,$(R)_4$-**L4**·[Lu]}) reflects the similarity between the glycol-linked and alkyl chain-linked environments after closure by RCM.

Knot Λ-**1**·[Lu] was readily demetalated by tetraethylammonium fluoride to give wholly organic knot Λ-**1** (Scheme S9). To confirm the absence of alternative entangled species, the reaction was also carried through all three steps from the ligand precursors to Λ-**1** without purification of the intermediates or final product. The matrix-assisted laser desorption/ionization (MALDI) spectrum of the crude reaction mixture after the final step features only ions corresponding to Λ-**1** (*m*/*z* [Λ-**1** + Na]$^+$ 1926.3, [Λ-**1** + K]$^+$ 1942.0, Figure S6). The absence of homomeric side products after kinetic trapping of the compound by RCM highlights the effectiveness of entropy-driven error correction in the system.

The demetalated knot Λ-**1** was subsequently isolated by size exclusion chromatography in overall 35% yield over three steps (Figure 2a). The ^{1}H NMR spectrum of Λ-**1** is broad and typical of other molecular knots that have no single well-defined conformation (Figure 2b(v)).[2] The metalated knot Λ-**1**·[Lu] could be smoothly regenerated (94% yield) by treatment of Λ-**1** with one equivalent of lutetium(III) trifluoromethanesulfonate in acetonitrile at 80 °C (Scheme S9).

Social Self-Sorting Synthesis of Composite Knots with Chiral Ditopic and Tetratopic Building Blocks. The applicability of the social self-sorting approach to more complex systems was then explored in the formation of a granny knot complex directly from two different chiral ligands. Ditopic ligand $(R)_4$-**L4** and tetratopic ligand $(R)_8$-**L5** were treated with lutetium(III) trifluoromethanesulfonate in a 1:1:2 ratio (Figure 3a). After 24 h, the ESI mass spectrum showed several ions corresponding to a heteromeric complex (*m*/*z* (Λ,Λ)-{$(R)_4$-**L4**,$(R)_8$-**L5**·$[Lu]_2$}$^{6+}$ 694.8, (Λ,Λ)-{$(R)_4$-**L4**,$(R)_8$-**L5**·$[Lu]_2$}$[CF_3SO_3]^{5+}$ 863.4, (Λ,Λ)-{$(R)_4$-**L4**,$(R)_8$-**L5**·$[Lu]_2$}$[CF_3SO_3]_2^{4+}$ 1116.4, (Λ,Λ)-{$(R)_4$-**L4**,$(R)_8$-**L5**·$[Lu]_2$}-$[CF_3SO_3]_3^{3+}$ 1538.2, Figure S89). Other ions in the spectrum correspond to overhand knot fragments containing a single non-coordinated ligand site, as observed previously for related open Vernier lanthanide complexes.[18b] The complex consisting of just one tetratopic ligand (*m*/*z* Λ-$(R)_8$-**L5**·$[Lu]^{3+}$ 901.3, Λ-$(R)_8$-**L5**·[Lu]$[CF_3SO_3]^{2+}$ 1425.9) can result from fragmentation of either the heteromeric granny knot or the Vernier template triskelion assembly. However, the complex consisting of two ditopic ligands (*m*/*z* Λ-$(($R$)_4$-**L4**$)_2$·$[Lu]^{3+}$ 918.0, Λ-$(($R$)_4$-**L4**$)_2$·[Lu]$[CF_3SO_3]^{2+}$ 1450.8) can only arise from fragmentation of the heteromeric granny complex. The ^{1}H

https://doi.org/10.1021/jacs.2c07682
J. Am. Chem. Soc. 2022, 144, 17232−17240

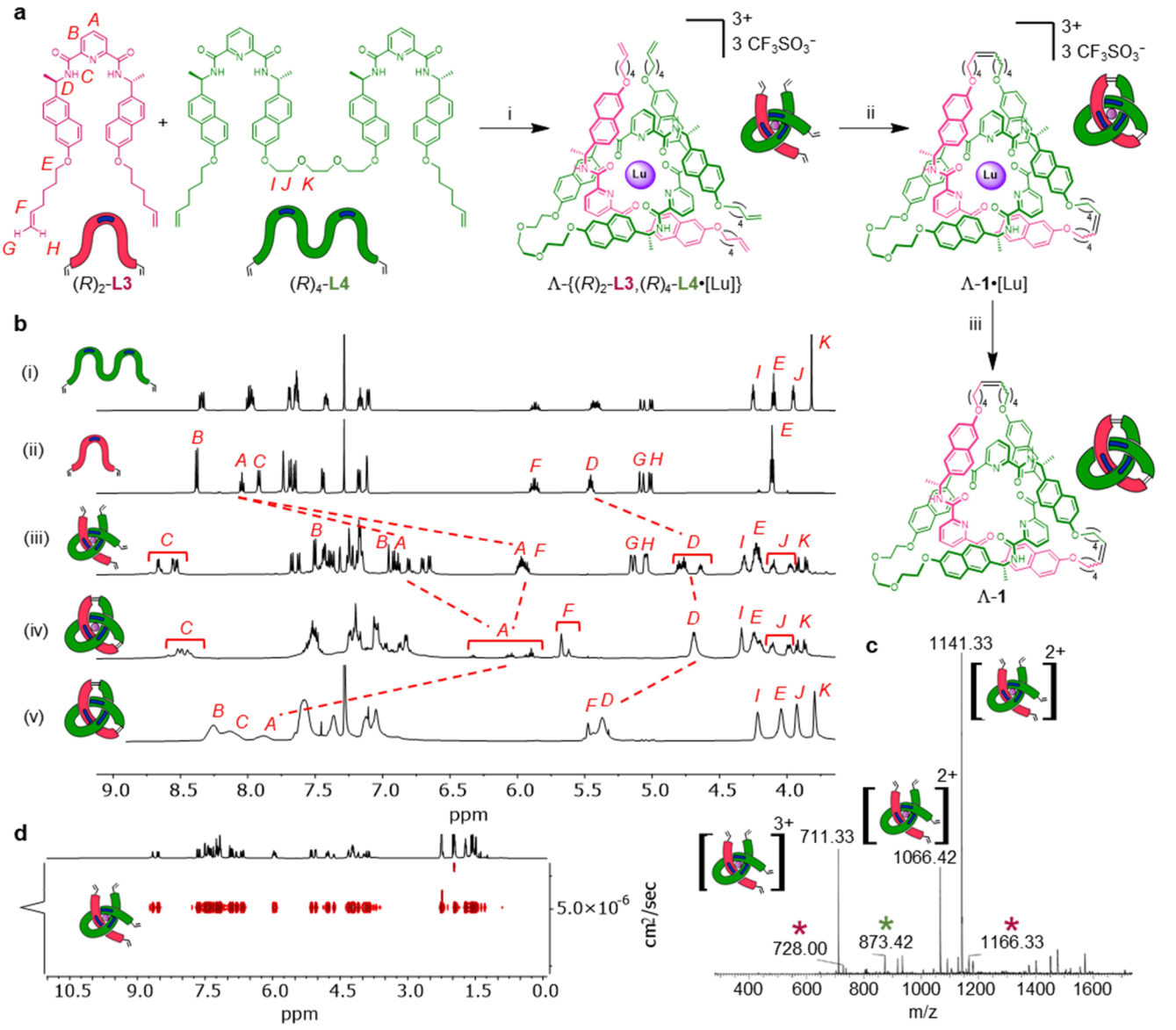

Figure 2. Socially self-sorted assembly of a trefoil knot of single topological handedness. (a) Synthesis of trefoil knot Λ-**1**. Reagents and conditions: (i) $Lu(CF_3SO_3)_3$, MeCN, 80 °C, 24 h. (ii) Hoveyda−Grubbs second generation catalyst,[16] CH_2Cl_2/CH_3NO_2 1:1 (v/v), 50 °C, 24 h, 53% over two steps. (iii) Et_4NF, MeCN, r.t., 0.5 h, 35% over three steps. Stereochemistry indicated by dark blue bars (*R*-stereocenters) on the cartoon representations of the ligand strands. (b) Partial ^1H NMR spectral stack plot of trefoil knot Λ-**1** and precursors (600 MHz, 298 K): (i) ligand $(R)_4$-**L4** ($CDCl_3$), (ii) ligand $(R)_2$-**L3** ($CDCl_3$), (iii) open trefoil knot complex Λ-{$(R)_2$-**L3**,$(R)_4$-**L4**·[Lu]} (MeCN-d_3), (iv) metalated knot Λ-**1**·[Lu] (MeCN-d_3), and (v) metal-free knot Λ-**1** ($CDCl_3$). Proton assignments refer to atom labels in part (a). For full assignments, see Supporting Information. (c) Low resolution ESI-MS(+) of a crude open trefoil knot complex mixture, showing major signals corresponding to Λ-{$(R)_2$-**L3**, $(R)_4$-**L4**·[Lu]}, and small signals corresponding to homomeric complexes Λ-$((R)_2$-**L3**$)_3$·[Lu] (pink *) and (Λ,Λ)-$((R)_4$-**L4**$)_3$·$[Lu]_2$ (green *). (d) DOSY ^1H NMR spectrum of open trefoil knot complex Λ-{$(R)_2$-**L3**,$(R)_4$-**L4**·[Lu]} (600 MHz, 298 K, MeCN-d_3), showing a single species is present in solution.

NMR spectrum shows shifts characteristic of strand entanglement [Figure 3(bi−iii)) and additional small signals which correspond to residual unbound ligand even after prolonged reaction times (signals marked *).

The alkene end groups of complex (Λ,Λ)-{$(R)_4$-**L4**,$(R)_8$-**L5**·$[Lu]_2$} were joined by RCM and the resulting closed-loop knot demetalated by treatment with Et_4NF (Figure 3a).[14b,15] As with trefoil knot Λ-**1**, the three steps to granny knot (Λ,Λ)-**2** were also undertaken without isolation of the intermediates to examine the efficacy of the self-sorting. We found no evidence of alternative homomeric products in the mass spectrum of the metalated (Figure S8) or demetalated (Figure S11) crude reaction mixtures, although a trefoil-entangled side product derived from intramolecular closure of fragment Λ-$(R)_8$-**L5**·[Lu] was observed throughout. The demetalated granny knot was isolated by size exclusion chromatography, yielding (Λ,Λ)-**2** in 13% yield over three steps (Scheme S11). The metalated knot (Λ,Λ)-**2**·$[Lu]_2$ could be isolated either after purification by size exclusion chromatography in 26% yield in two steps from $(R)_4$-**L4** and $(R)_8$-**L5** (Figure 3a) or in 68% yield by remetalation of (Λ,Λ)-**2** (Scheme S11).

The molecular masses of (Λ,Λ)-**2**·$[Lu]_2$ and (Λ,Λ)-**2** were confirmed by HRMS (Figure 3c) and MALDI-TOF (Figure S97), respectively. The ^1H NMR spectrum of (Λ,Λ)-**2**·$[Lu]_2$

https://doi.org/10.1021/jacs.2c07682
J. Am. Chem. Soc. 2022, 144, 17232−17240

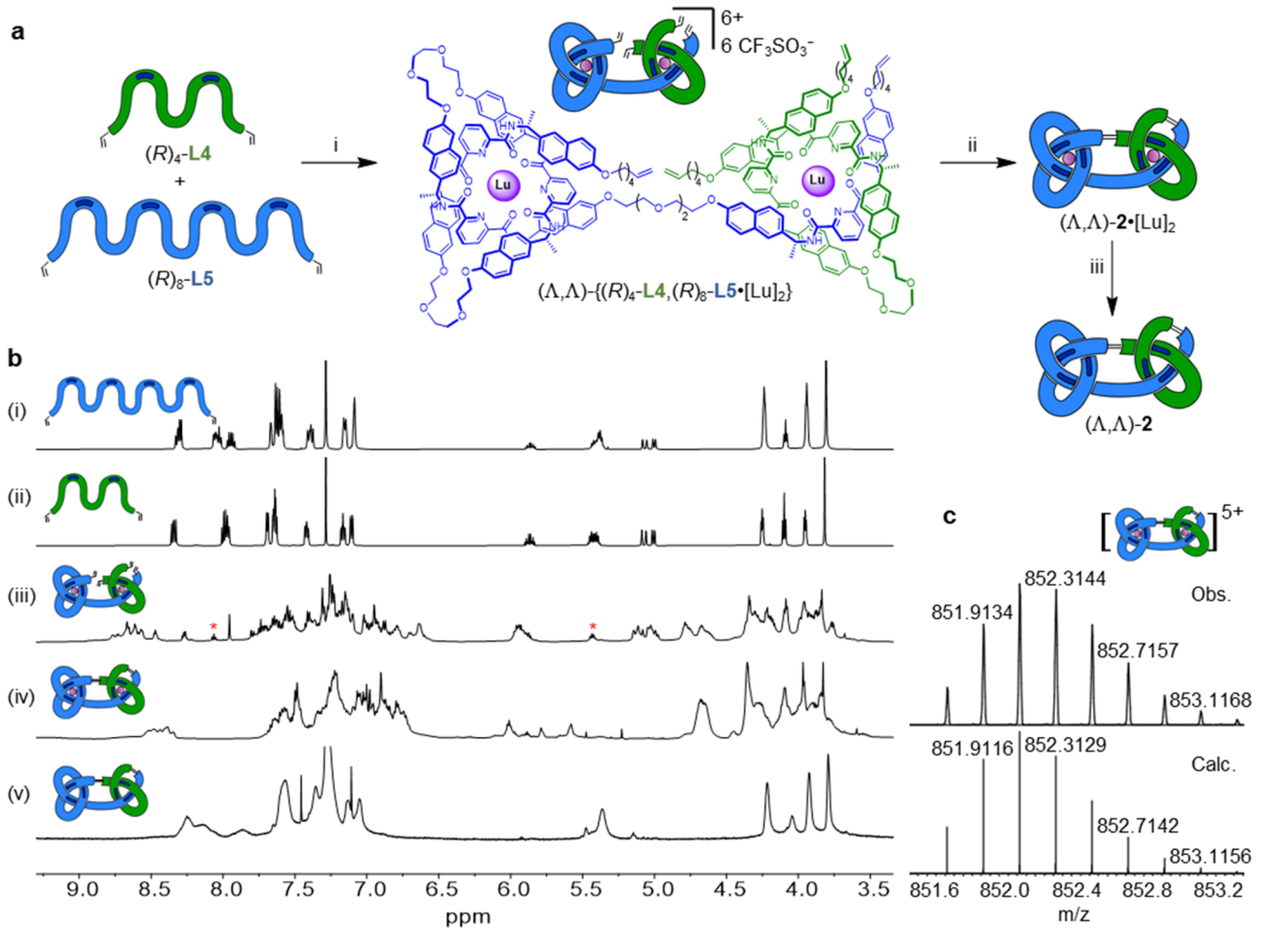

Figure 3. Socially self-sorted assembly of a granny knot of single topological handedness. (a) Synthesis of granny knot (Λ,Λ)-**2**. Reagents and conditions: (i) $Lu(CF_3SO_3)_3$, MeCN, 80 °C, 72 h. (ii) Hoveyda−Grubbs second generation catalyst, CH_2Cl_2/CH_3NO_2 1:1 (v/v), 50 °C, 24 h, 26% over two steps. (iii) Et_4NF, MeCN, r.t., 0.5 h, 13% over three steps. (b) Partial ^1H NMR spectral stack plot of granny knot (Λ,Λ)-**2** and precursors (600 MHz, 298 K): (i) ligand $(R)_8$-**L5** ($CDCl_3$), (ii) ligand $(R)_4$-**L4** ($CDCl_3$), (iii) open granny knot complex (Λ,Λ)-{$(R)_4$-**L4**,$(R)_8$-**L5**·$[Lu]_2$} (MeCN-d_3), (iv) metalated knot (Λ,Λ)-**2**·$[Lu]_2$ (MeCN-d_3), and (v) metal-free granny knot (Λ,Λ)-**2** ($CDCl_3$). Uncoordinated ligand impurities are indicated *. For full assignments, see Supporting Information. (c) High-resolution ESI-MS(+) of closed-loop granny knot (Λ,Λ)-**2**·$[Lu]_2$, comparing the observed spectrum (above) to calculated isotopic distribution of $[M - 5(CF_3SO_3)]^{5+}$ (below).

(Figure 3b(iv)) is similar to that of previously reported composite knots,[20,21] and the ^1H NMR spectrum of the demetalated knot (Λ,Λ)-**2** is broad (Figure 3b(v)).

Social Self-Sorting of Pre-Coordinated Entangled Strands under Thermodynamic Control. The dynamic conversion of entangled complexes was also investigated (Figure 4a). Equimolar solutions of homomeric helicate Λ-$((R)_2$-**L3**$)_3$·[Lu] and open granny knot complex (Λ,Λ)-$((R)_4$-**L4**$)_3$·$[Lu]_2$ in MeCN were mixed, and the evolution of heteromeric complex Λ-{$(R)_2$-**L3**,$(R)_4$-**L4**·[Lu]} was monitored by ^1H NMR spectroscopy and ESI mass spectrometry. Within 10 min at room temperature, ions corresponding to Λ-{$(R)_2$-**L3**,$(R)_4$-**L4**·[Lu]} became apparent by mass spectrometry, becoming the dominant species after 4 h at 80 °C (Figure 4b). Near-complete conversion to the heteromeric socially self-sorted complex was qualitatively confirmed by ^1H NMR spectroscopy (Figure 4c). The dynamic rearrangement of preformed complexes to an entropically favored heteromeric compound was also qualitatively shown by an equimolar mixture of granny knot complex (Λ,Λ)-$((R)_4$-**L4**$)_3$·$[Lu]_2$ and triskelion knot complex (Λ_3,Λ)-$((R)_8$-**L5**$)_3$·$[Lu]_4$ (see Section S4.7).

Control of Entanglement Stereochemistry with Building Block Point Chirality. Monotopic pdc lanthanide helicates containing either (*R*)- or (*S*)-stereogenic centers do not self-sort on the basis of chirality.[15] However, covalently tethered tritopic ligands containing four (*R*)- and two (*S*)-stereocenters do not self-entangle upon coordination to lanthanide(III) ions because of steric clashes arising from the strand stereochemistry.[18b] We therefore explored combining stereochemical discrimination and entropically driven social self-sorting in order to prepare a composite knot containing tangles of opposing handedness. Ditopic ligand $(S)_4$-**L4** and tetratopic ligand $(S)_2(R)_6$-**L5** were synthesized as previously reported.[18b] The combination of six stereocenters of (*R*)-chirality and six of (*S*)-chirality across the two ligands is required for forming two trefoil tangles of opposing handedness, a $3_1\#^*3_1$ "square knot" (Λ,Δ)-**2**, and a diastereomer of granny knot (Λ,Λ)-**2** (Schemes S10 and S12).

To assemble square knot (Λ,Δ)-**2**, a 1:1:2 mixture of tetratopic ligand $(S)_2(R)_6$-**L5**, ditopic ligand $(S)_4$-**L4** and lutetium(III) trifluoromethanesulfonate in acetonitrile afforded open square knot complex (Λ,Δ)-{$(S)_4$-**L4**,$(S)_2(R)_6$-**L5**·$[Lu]_2$} after heating at 80 °C for 72 h (Figure 5a). Its mass spectrum

https://doi.org/10.1021/jacs.2c07682
J. Am. Chem. Soc. 2022, 144, 17232−17240

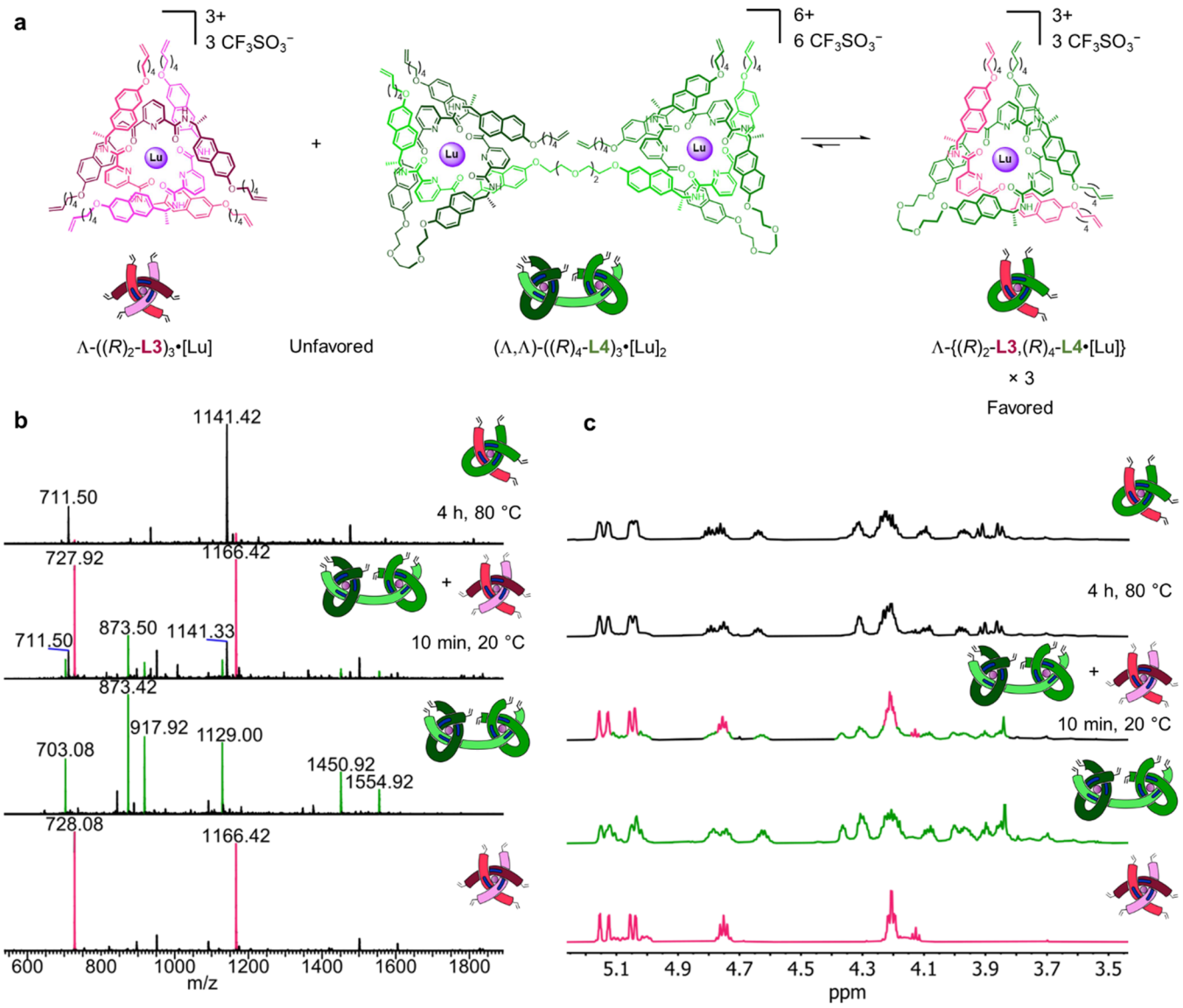

Figure 4. Socially self-sorted rearrangement of complexes to give a heteromeric complex of single entanglement stereochemistry. (a) Synthesis of heteromeric complex Λ-{$(R)_2$-**L3**,$(R)_4$-**L4**·[Lu]}. Reagents and conditions: MeCN, 80 °C, 4 h. (b) Comparison of precursor complexes and (qualitative) in situ monitoring of rearrangement by ESI(+) mass spectrometry. (c) Comparison of precursor complexes and (qualitative) in situ monitoring of rearrangement by ^{1}H NMR spectroscopy (600 MHz, 298 K, MeCN-d_3), including a reference sample of pristine heteromeric complex Λ-{$(R)_2$-**L3**,$(R)_4$-**L4**·[Lu]} (top).

was similar to that of the diastereomeric granny knot complex (Λ,Λ)-{$(R)_4$-**L4**,$(R)_8$-**L5**·$[Lu]_2$} (Figure S93). Complex (Λ,Δ)-{$(S)_4$-**L4**,$(S)_2(R)_6$-**L5**·$[Lu]_2$} is pseudo-achiral, particularly in terms of the environment and stereochemistry of the point-chiral centers around each coordinated Lu(III) ion, and accordingly gives a near baseline CD spectrum (Figure S122). Joining of the terminal alkenes of (Λ,Δ)-{$(S)_4$-**L4**,$(S)_2(R)_6$-**L5**·$[Lu]_2$} by RCM gave square knot (Λ,Δ)-**2**·$[Lu]_2$ (Scheme S12). Subsequent demetalation by Et_4NF afforded square knot (Λ,Δ)-**2** in 7% yield over three steps (Scheme S13).

Square knot (Λ,Δ)-**2**·$[Lu]_2$ and granny knot (Λ,Λ)-**2**·$[Lu]_2$ have virtually indistinguishable ^{1}H NMR spectra (Figures S60 and S64) but strikingly different CD responses (Figure 5b). The small deviations from the baseline in the CD spectrum of (Λ,Δ)-**2**·$[Lu]_2$ are likely the result of the different connectivities of the point-chiral groups on the strand.

CONCLUSIONS

Our findings demonstrate that molecular prime and composite knots can be rapidly assembled by social self-sorting using 2,6-pyridinedicarboxamide-containing strands of different topicity. A 1:1 ratio of monotopic and ditopic pdc ligands coordinates to Lu(III) to selectively generate a heteromeric precursor complex to a trefoil knot. Molecular granny and square knots can be assembled through social self-sorting of chiral ditopic and tetratopic ligand strands. The pdc-Ln(III) social self-sorting is dynamic, with pre-coordinated lanthanide complexes of the ligand strands rapidly rearranging to the entropically preferred self-sorted structures. Social self-sorting of programed pdc-ligand strands is a highly effective new addition to the strategies[10−13,18] available for the rapid assembly of well-defined sequences of orderly molecular entanglements. The ability to access low-symmetry knots with simpler synthetic

https://doi.org/10.1021/jacs.2c07682
J. Am. Chem. Soc. 2022, 144, 17232−17240

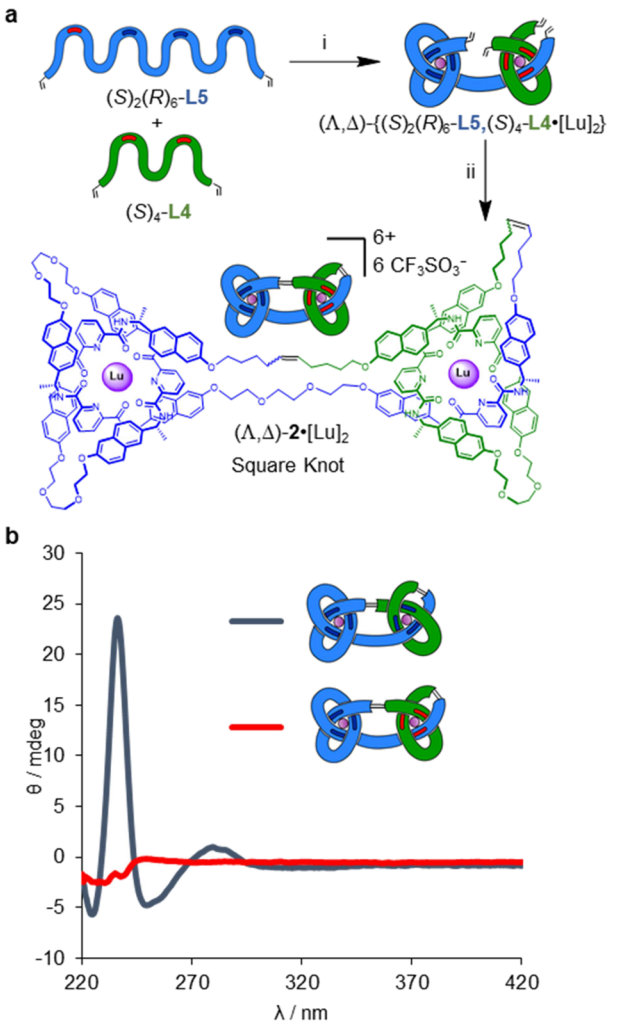

Figure 5. Socially self-sorted assembly of a square knot (*meso*-topological handedness). (a) Synthesis of square knot (Λ,Δ)-**2**·$[Lu]_2$. Reagents and conditions: (i) $Lu(CF_3SO_3)_3$, MeCN, 80 °C, 72 h. (ii) Hoveyda–Grubbs second generation catalyst,[16] CH_2Cl_2/CH_3NO_2 1:1 (v/v), 50 °C, 24 h, 29% over two steps. (b) CD spectral stack plot (5×10^{-5} M, MeCN, normalized for absorbance) showing comparison of granny knot (Λ,Λ)-**2**·$[Lu]_2$ (blue) and square knot (Λ,Δ)-**2**·$[Lu]_2$ (red).

strategies provides new avenues to explore the functions and properties associated with molecular entanglements.

■ ASSOCIATED CONTENT

Supporting Information

The Supporting Information is available free of charge at https://pubs.acs.org/doi/10.1021/jacs.2c07682.

Additional experimental details including synthetic procedures and characterization data (PDF)

■ AUTHOR INFORMATION

Corresponding Author

David A. Leigh – *Department of Chemistry, University of Manchester, Manchester M13 9PL, U.K.; School of Chemistry and Molecular Engineering, East China Normal University, Shanghai 200062, China;* orcid.org/0000-0002-1202-4507; Email: david.leigh@manchester.ac.uk

Authors

Zoe Ashbridge – *Department of Chemistry, University of Manchester, Manchester M13 9PL, U.K.*

Olivia M. Knapp – *Department of Chemistry, University of Manchester, Manchester M13 9PL, U.K.;* orcid.org/0000-0003-0670-2305

Elisabeth Kreidt – *Department of Chemistry, University of Manchester, Manchester M13 9PL, U.K.*

Lucian Pirvu – *Department of Chemistry, University of Manchester, Manchester M13 9PL, U.K.*

Fredrik Schaufelberger – *Department of Chemistry, University of Manchester, Manchester M13 9PL, U.K.;* orcid.org/0000-0001-5298-4310

Complete contact information is available at: https://pubs.acs.org/10.1021/jacs.2c07682

Notes

The authors declare no competing financial interest.

■ ACKNOWLEDGMENTS

We thank the Engineering and Physical Sciences Research Council (EPSRC; EP/P027067/1), the European Research Council (ERC; Advanced Grant 786630), the Marie Skłodowska-Curie Actions of the European Union (Individual Postdoctoral Fellowship to F.S., EC 746993), and the German Research Foundation (DFG, Individual Postdoctoral Fellowship to E.K.) for funding. We thank the University of Manchester Mass Spectrometry Service Center for high-resolution mass spectrometry and MALDI-TOF. D.A.L. is a Royal Society Research Professor.

■ ABBREVIATIONS

OTf	trifluoromethanesulfonate
pdc	2,6-pyridinedicarboxamide
MALDI	matrix-assisted laser desorption/ionization
RCM	ring-closing olefin metathesis
r.t.	room temperature.

■ REFERENCES

(1) (a) Adams, C. C. *The Knot Book: An Elementary Introduction to the Mathematical Theory of Knots*; American Mathematical Society: Providence, RI, 2004. (b) Lim, N. C. H.; Jackson, S. E. Molecular knots in biology and chemistry. *J. Phys.: Condens. Matter* **2015**, *27*, No. 354101. (c) Fielden, S. D. P.; Leigh, D. A.; Woltering, S. L. Molecular knots. *Angew. Chem., Int. Ed.* **2017**, *56*, 11166–11194. (d) Guo, Q.; Jiao, Y.; Feng, Y.; Stoddart, J. F. The rise and promise of molecular nanotopology. *CCS Chem.* **2021**, *3*, 1542–1572. (e) Ashbridge, Z.; Fielden, S. D. P.; Leigh, D. A.; Pirvu, L.; Schaufelberger, F.; Zhang, L. Knotting matters: Orderly molecular entanglements. *Chem. Soc. Rev.* **2022**, Advance Article DOI: 10.1039/d2cs00323f.

(2) Leigh, D. A.; Schaufelberger, F.; Pirvu, L.; Halldin Stenlid, J.; August, D. P.; Segard, J. Tying different knots in a molecular strand. *Nature* **2020**, *584*, 562–568.

(3) Saitta, A. M.; Soper, P. D.; Wasserman, E.; Klein, M. L. Influence of a knot on the strength of a polymer strand. *Nature* **1999**, *399*, 46–48.

(4) (a) Zhang, L.; Lemonnier, J.-F.; Acocella, A.; Calvaresi, M.; Zerbetto, F.; Leigh, D. A. Effects of knot tightness at the molecular level. *Proc. Natl. Acad. Sci. U. S. A.* **2019**, *116*, 2452–2457. (b) Song, Y.; Schaufelberger, F.; Ashbridge, Z.; Pirvu, L.; Vitorica-Yrezabal, I. J.; Leigh, D. A. Effects of turn-structure on folding and entanglement in artificial molecular overhand knots. *Chem. Sci.* **2021**, *12*, 1826–1833.

(5) Caprice, K.; Aster, A.; Cougnon, F. B. L.; Kumpulainen, T. Untying the photophysics of quinolinium-based molecular knots and links. *Chem. – Eur. J.* **2020**, *26*, 1576–1587.
(6) (a) Marcos, V.; Stephens, A. J.; Jaramillo-Garcia, J.; Nussbaumer, A. L.; Woltering, S. L.; Valero, A.; Lemonnier, J.-F.; Vitorica-Yrezabal, I. J.; Leigh, D. A. Allosteric initiation and regulation of catalysis with a molecular knot. *Science* **2016**, *352*, 1555–1559. (b) Prakasam, T.; Devaraj, A.; Saha, R.; Lusi, M.; Brandel, J.; Esteban-Gómez, D.; Platas-Iglesias, C.; Olson, M. A.; Mukherjee, P. S.; Trabolsi, A. Metal–organic self-assembled trefoil knots for C—Br bond activation. *ACS Catal.* **2019**, *9*, 1907–1914.
(7) Leigh, D. A.; Pirvu, L.; Schaufelberger, F.; Tetlow, D. J.; Zhang, L. Securing a supramolecular architecture by tying a stopper knot. *Angew. Chem., Int. Ed.* **2018**, *57*, 10484–10488.
(8) Katsonis, N.; Lancia, F.; Leigh, D. A.; Pirvu, L.; Ryabchun, A.; Schaufelberger, F. Knotting a molecular strand can invert macroscopic effects of chirality. *Nat. Chem.* **2020**, *12*, 939–944.
(9) (a) Benyettou, F.; Prakasam, T.; Ramdas Nair, A.; Witzel, I.-I.; Alhashimi, M.; Skorjanc, T.; Olsen, J.-C.; Sadler, K. C.; Trabolsi, A. Potent and selective in vitro and in vivo antiproliferative effects of metal–organic trefoil knots. *Chem. Sci.* **2019**, *10*, 5884–5892. (b) August, D. P.; Borsley, S.; Cockroft, S. L.; della Sala, F.; Leigh, D. A.; Webb, S. J. Transmembrane ion channels formed by a Star of David [2]catenane and a molecular pentafoil knot. *J. Am. Chem. Soc.* **2020**, *142*, 18859–18865.
(10) (a) Dietrich-Buchecker, C. O.; Sauvage, J.-P. A synthetic molecular trefoil knot. *Angew. Chem., Int. Ed.* **1989**, *28*, 189–192. (b) Dietrich-Buchecker, C. O.; Guilhem, J.; Pascard, C.; Sauvage, J.-P. Structure of a synthetic trefoil knot coordinated to two copper(I) centers. *Angew. Chem., Int. Ed.* **1990**, *29*, 1154–1156. (c) Safarowsky, O.; Nieger, M.; Fröhlich, R.; Vögtle, F. A molecular knot with twelve amide groups — one-step synthesis, crystal structure, chirality. *Angew. Chem., Int. Ed.* **2000**, *39*, 1616–1618. (d) Feigel, M.; Ladberg, R.; Engels, S.; Herbst-Irmer, R.; Fröhlich, R. A trefoil knot made of amino acids and steroids. *Angew. Chem., Int. Ed.* **2006**, *45*, 5698–5702. (e) Barran, P. E.; Cole, H. L.; Goldup, S. M.; Leigh, D. A.; McGonigal, P. R.; Symes, M. D.; Wu, J.; Zengerle, M. Active-metal template synthesis of a molecular trefoil knot. *Angew. Chem., Int. Ed.* **2011**, *50*, 12280–12284.
(11) (a) Ponnuswamy, N.; Cougnon, F. B. L.; Clough, J. M.; Pantoş, G. D.; Sanders, J. K. M. Discovery of an organic trefoil knot. *Science* **2012**, *338*, 783–785. (b) Cougnon, F. B. L.; Caprice, K.; Pupier, M.; Bauzá, A.; Frontera, A. A strategy to synthesize molecular knots and links using the hydrophobic effect. *J. Am. Chem. Soc.* **2018**, *140*, 12442–12450.
(12) (a) Prakasam, T.; Lusi, M.; Elhabiri, M.; Platas-Iglesias, C.; Olsen, J. C.; Asfari, Z.; Cianférani-Sanglier, S.; Debaene, F.; Charbonnière, L. J.; Trabolsi, A. Simultaneous self-assembly of a [2]catenane, a trefoil knot, and a Solomon Link from a simple pair of ligands. *Angew. Chem., Int. Ed.* **2013**, *52*, 9956–9960. (b) Prakasam, T.; Bilbeisi, R. A.; Lusi, M.; Olsen, J.-C.; Platas-Iglesias, C.; Trabolsi, A. Post-synthetic modifications of cadmium-based knots and links. *Chem. Commun.* **2016**, *52*, 7398–7401. (c) Bilbeisi, R. A.; Prakasam, T.; Lusi, M.; El Khoury, R.; Platas-Iglesias, C.; Charbonnière, L. J.; Olsen, J. C.; Elhabiri, M.; Trabolsi, A. [C-H···Anion] interactions mediate the templation and anion binding properties of topologically non-trivial metal-organic structures in aqueous solutions. *Chem. Sci.* **2016**, *7*, 2524–2531.
(13) (a) Ayme, J.-F.; Beves, J. E.; Leigh, D. A.; McBurney, R. T.; Rissanen, K.; Schultz, D. A synthetic molecular pentafoil knot. *Nat. Chem.* **2012**, *4*, 15–20. (b) Ayme, J.-F.; Beves, J. E.; Leigh, D. A.; McBurney, R. T.; Rissanen, K.; Schultz, D. Pentameric circular iron(II) double helicates and a molecular pentafoil knot. *J. Am. Chem. Soc.* **2012**, *134*, 9488–9497. (c) Danon, J. J.; Krüger, A.; Leigh, D. A.; Lemonnier, J.-F.; Stephens, A. J.; Vitorica-Yrezabal, I. J.; Woltering, S. L. Braiding a molecular knot with eight crossings. *Science* **2017**, *355*, 159–162. (d) Zhang, L.; August, D. P.; Zhong, J.; Whitehead, G. F. S.; Vitorica-Yrezabal, I. J.; Leigh, D. A. A molecular trefoil knot from a trimeric circular helicate. *J. Am. Chem. Soc.* **2018**, *140*, 4982–4985. (e) Leigh, D. A.; Danon, J. J.; Fielden, S. D. P.; Lemonnier, J.-F.; Whitehead, G. F. S.; Woltering, S. L. A molecular endless (7_4) knot. *Nat. Chem.* **2021**, *13*, 117–122. (f) Carpenter, J. P.; McTernan, C. T.; Greenfield, J. L.; Lavendomme, R.; Ronson, T. K.; Nitschke, J. R. Controlling the shape and chirality of an eight-crossing molecular knot. *Chem* **2021**, *7*, 1534–1543.
(14) (a) Leonard, J. P.; Jensen, P.; McCabe, T.; O'Brien, J. E.; Peacock, R. D.; Kruger, P. E.; Gunnlaugsson, T. Self-assembly of chiral luminescent lanthanide coordination bundles. *J. Am. Chem. Soc.* **2007**, *129*, 10986–10987. (b) Ayme, J.-F.; Gil-Ramírez, G.; Leigh, D. A.; Lemonnier, J.-F.; Markevicius, A.; Muryn, C. A.; Zhang, G. Lanthanide template synthesis of a molecular trefoil knot. *J. Am. Chem. Soc.* **2014**, *136*, 13142–13145.
(15) Zhang, G.; Gil-Ramírez, G.; Markevicius, A.; Browne, C.; Vitorica-Yrezabal, I. J.; Leigh, D. A. Lanthanide template synthesis of trefoil knots of single handedness. *J. Am. Chem. Soc.* **2015**, *137*, 10437–10442.
(16) Garber, S. B.; Kingsbury, J. S.; Gray, B. L.; Hoveyda, A. H. Efficient and recyclable monomeric and dendritic Ru-based metathesis catalysts. *J. Am. Chem. Soc.* **2000**, *122*, 8168–8179.
(17) (a) Adams, H.; Ashworth, E.; Breault, G. A.; Guo, J.; Hunter, C. A.; Mayers, P. C. Knot tied around an octahedral metal center. *Nature* **2001**, *411*, 763. (b) Guo, J.; Mayers, P. C.; Breault, G. A.; Hunter, C. A. Synthesis of a molecular trefoil knot by folding and closing on an octahedral coordination template. *Nat. Chem.* **2010**, *2*, 218–222.
(18) (a) Gil-Ramírez, G.; Hoekman, S.; Kitching, M. O.; Leigh, D. A.; Vitorica-Yrezabal, I. J.; Zhang, G. Tying a molecular overhand knot of single handedness and asymmetric catalysis with the corresponding pseudo-D_3-symmetric trefoil knot. *J. Am. Chem. Soc.* **2016**, *138*, 13159–13162. (b) Ashbridge, Z.; Kreidt, E.; Pirvu, L.; Schaufelberger, F.; Halldin Stenlid, J.; Abild-Pedersen, F.; Leigh, D. A. Vernier template synthesis of molecular knots. *Science* **2022**, *375*, 1035–1041.
(19) Carina, R. F.; Dietrich-Buchecker, C.; Sauvage, J.-P. Molecular composite knots. *J. Am. Chem. Soc.* **1996**, *118*, 9110–9116.
(20) Leigh, D. A.; Pirvu, L.; Schaufelberger, F. Stereoselective synthesis of molecular square and granny knots. *J. Am. Chem. Soc.* **2019**, *141*, 6054–6059.
(21) (a) Danon, J. J.; Leigh, D. A.; Pisano, S.; Valero, A.; Vitorica-Yrezabal, I. J. A six-crossing doubly interlocked [2]catenane with twisted rings, and a molecular granny knot. *Angew. Chem., Int. Ed.* **2018**, *57*, 13833–13837. (b) Zhang, L.; Stephens, A. J.; Nussbaumer, A. L.; Lemonnier, J.-F.; Jurček, P.; Vitorica-Yrezabal, I. J.; Leigh, D. A. Stereoselective synthesis of a composite knot with nine crossings. *Nat. Chem.* **2018**, *10*, 1083–1088.
(22) (a) Safont-Sempere, M. M.; Fernández, G.; Würthner, F. Self-sorting phenomena in complex supramolecular systems. *Chem. Rev.* **2011**, *111*, 5784–5814. (b) Ludlow, R. F.; Otto, S. Systems chemistry. *Chem. Soc. Rev.* **2008**, *37*, 101–108.
(23) (a) Kramer, R.; Lehn, J.-M.; Marquis-Rigault, A. Self-recognition in helicate self-assembly: Spontaneous formation of helical metal complexes from mixtures of ligands and metal ions. *Proc. Natl. Acad. Sci. U. S. A.* **1993**, *90*, 5394–5398. (b) Ayme, J.-F.; Beves, J. E.; Campbell, C. J.; Leigh, D. A. The self-sorting behavior of circular helicates and molecular knots and links. *Angew. Chem., Int. Ed.* **2014**, *53*, 7823–7827. (c) Zhong, J.; Zhang, L.; August, D. P.; Whitehead, G. F. S.; Leigh, D. A. Self-sorting assembly of molecular trefoil knots of single handedness. *J. Am. Chem. Soc.* **2019**, *141*, 14249–14256.
(24) (a) Mukhopadhyay, P.; Wu, A.; Isaacs, L. Social self-sorting in aqueous solution. *J. Org. Chem.* **2004**, *69*, 6157–6164. (b) He, Z.; Jiang, W.; Schalley, C. A. Integrative self-sorting: A versatile strategy for the construction of complex supramolecular architecture. *Chem. Soc. Rev.* **2015**, *44*, 779–789. (c) Bloch, W. M.; Clever, G. H. Integrative self-sorting of coordination cages based on 'naked' metal ions. *Chem. Commun.* **2017**, *53*, 8506–8516. (d) Greenaway, R. L.; Santolini, V.; Pulido, A.; Little, M. A.; Alston, B. M.; Briggs, M. E.; Day, G. M.; Cooper, A. I.; Jelfs, K. E. From concept to crystals via prediction: multi-component organic cage pots by social self-sorting.

https://doi.org/10.1021/jacs.2c07682
J. Am. Chem. Soc. 2022, 144, 17232–17240

Angew. Chem., Int. Ed. **2019**, *58*, 16275−16281. (e) Han, K.; Go, D.; Tigges, T.; Rahimi, K.; Kuehne, A. J. C.; Walther, A. Social self-sorting of colloidal families in co-assembling microgel systems. *Angew. Chem., Int. Ed.* **2017**, *129*, 2208−2214. (f) Coubrough, H. M.; van der Lubbe, S. C. C.; Hetherington, K.; Minard, A.; Pask, C.; Howard, M. J.; Fonseca Guerra, C.; Wilson, A. J. Supramolecular self-sorting networks using hydrogen-bonding motifs. *Chem. − Eur. J.* **2018**, *25*, 785−795.

(25) Wu, A.; Isaacs, L. Self-sorting: the exception or the rule? *J. Am. Chem. Soc.* **2003**, *125*, 4831−4835.

(26) De, S.; Mahata, K.; Schmittel, M. Metal-coordination-driven dynamic heteroleptic architectures. *Chem. Soc. Rev.* **2010**, *39*, 1555−1575.

https://doi.org/10.1021/jacs.2c07682
J. Am. Chem. Soc. 2022, 144, 17232−17240